

# Deformation zones and entanglements in glassy polymers\*

Athene M. Donald† and Edward J. Kramer

Department of Materials Science and Engineering and the Materials Science Center,  
Cornell University, Ithaca, New York, 14853, USA

(Received 14 September 1981)

Deformation zones are regions of drawn but unfractured material which grow from crack tips in thin films of glassy polymers which have a low value of  $l_e$ , the chain contour length between entanglements. The growth of these zones is observed optically and their final structure characterized by transmission electron microscopy. By microdensitometry of the electron image plate the average value of the extension ratio within the deformation zone,  $\lambda_{DZ}$ , is measured. Such deformation zones have been grown in thin films of four homopolymers and a series of polymer blends. It is found that  $\lambda_{DZ}$  is approximately  $0.6 \lambda_{max}$ , where  $\lambda_{max}$  is a predicted maximum extension ratio derived from a simple model in which the entanglement points are assumed to act as permanent crosslinks with no chain slippage or scission occurring. This value of  $\lambda_{DZ}$  is lower than the extension ratios previously measured for crazes grown in the same polymers; typical  $\lambda_{craze}$  values lie much closer to  $\lambda_{max}$ . This result can be rationalized by realizing that at least a limited degree of chain scission/slippage must occur during crazing to permit the generation of the void-fibril network. For those polymers where both crazing and deformation zones may form, the latter grow rapidly whereas the formation of crazes requires longer times. This observation also indicates the importance of the kinetic process of chain scission/chain slippage for crazing. Annealing of the polymer films below the glass transition temperature leads to an increased tendency for crazing relative to the growth of deformation zones.

**Keywords** Deformation zone; entanglements; extension ratio; transmission electron microscopy; shear; crazing

## INTRODUCTION

Crazes are commonly observed to form when glassy polymers are loaded under tension<sup>1-3</sup>. These crazes are planar defects which are load bearing by virtue of the array of fibrils which span the craze-matrix interfaces. The presence of this void-fibril network has been clearly revealed by transmission electron microscopy (TEM)<sup>4-9</sup>. Although crazes are load bearing and are a major source of toughness for thermoplastics, they also act as precursors to cracks which can form by fibril breakdown within the craze. The ease with which this breakdown may occur is strongly influenced by the extension ratio,  $\lambda$ , of the polymer within the craze, since, for a given level of stress on the craze surface  $S$ , the true fibril stress will be enhanced by a factor of  $\lambda$ .

A method for determining  $\lambda$  has been developed using quantitative transmission electron microscopy<sup>8</sup> and it has become possible to examine typical extension ratios for crazes in a wide range of glassy polymers<sup>10</sup> and polymer blends<sup>11</sup>. The results of these studies show a strong correlation between the values of  $\lambda$  experimentally measured for each polymer ( $\lambda_{craze}$ ) with the chain contour length between entanglements,  $l_e$ , obtained from melt elasticity measurements. In particular,  $\lambda_{craze}$  can be compared with the maximum value for the extension ratio  $\lambda_{max}$  predicted from a simple model in which entanglement points are assumed to act as permanent crosslinks, with

no chain slippage or scission occurring. In this case:

$$\lambda_{max} = l_e/d \quad (1)$$

where  $d$  is the root-mean-square end-to-end distance of a chain of molecular weight  $M_e$ , the entanglement molecular weight. The approximate value of  $d$  can be obtained from the variation of the radius of gyration with molecular weight as determined from small-angle neutron or light scattering experiments. The comparison of  $\lambda_{craze}$  with  $\lambda_{max}$  for the wide range of polymer systems studied (homopolymers, random copolymers and polymer blends) shows a strong correlation with the average value  $\lambda_{craze} \approx 0.8 \lambda_{max}$  for most systems<sup>10,11</sup>. For polymers with large  $l_e$  and large  $\lambda$ s such as poly(t-butylstyrene) (PTBS),  $\lambda_{craze}$  actually exceeds  $\lambda_{max}$ , suggesting a significant contribution from chain scission due to the high fibril stresses. The same effect is thought to cause the higher  $\lambda$  values measured within the midrib of crazes.

From these observations it is clear that polymers with large values of  $l_e$  which have very large, but localized ductility as measured by  $\lambda_{craze}$ , are rather 'brittle' in the conventional sense, since the high elongation within the crazes causes ready breakdown to form cracks. Alternatively, polymers with low values of  $l_e$  and  $\lambda_{craze}$  might be expected to be tougher, as is indeed the case for polycarbonate (PC) and poly(phenylene oxide) (PPO).

During the course of these investigations it became clear that for these polymers (with low  $l_e$ ) a second mode of plastic deformation occurs which could also contribute significantly to toughness. This process, which will

\* MSc Report No. 4550, Cornell University.

† Present address: Dept. of Metallurgy and Materials Science, Cambridge University, Pembroke St., Cambridge CB2 3QZ, UK.

compete with crazing under certain circumstances, involves shear and in thin films leads to the formation of plane stress deformation zones (DZs). These zones have been extensively characterized for PC<sup>12,13</sup> in which crazing is rarely observed to occur in the thin films suitable for study by TEM and optical microscopy methods.

The nature of these shear deformation zones is highly sensitive to physical ageing; in unaged specimens of PC an extensive and diffuse region of deformation is generated at a crack tip (as revealed by optical microscopy), but following a short annealing just below  $T_g$ , the glass transition temperature, the deformation becomes highly localized. Using the same methods for determining the craze extension ratios, TEM studies have shown that the extension ratio within the zones in annealed PC is essentially constant throughout at  $\lambda = 1.4$ .

Since it has been shown<sup>10,11</sup> in many polymers that the entanglement network is a major factor determining craze microstructure and strength, it may be anticipated that entanglements will also be important in determining the properties of these deformation zones.

Results on the nature of DZs in homopolymers and polymer blends of low  $l_e$  are presented here. Measurements of the extension ratio  $\lambda_{DZ}$  are compared with  $\lambda_{max}$ . The effects of ageing treatments on the competition between deformation zone and craze formation are also discussed.

## EXPERIMENTAL

Thin films ( $\sim 0.8 \mu\text{m}$ ) were prepared from solutions made by dissolving each polymer in an appropriate solvent. The polymer-solvent systems used were:

(1) Polycarbonate (PC) (Lexan<sup>TM</sup>) reactor powder with weight-average molecular weight,  $\bar{M}_w = 39\,000$  and number-average molecular weight,  $\bar{M}_n = 15\,700$ , dissolved in methylene chloride.

(2) Poly(2,6-dimethyl-1,4-phenylene oxide) (PPO<sup>TM</sup>) with  $\bar{M}_w = 35\,000$  and  $\bar{M}_n = 15\,000$ , dissolved in chloroform.

(3) Two types of polystyrene-acrylonitrile, a random copolymer: PSAN1 contained 76 wt% styrene and 24 wt% acrylonitrile with  $\bar{M}_w = 216\,000$  and  $\bar{M}_n = 102\,000$  and PSAN2 contained 34 wt% styrene with  $\bar{M}_w = 106\,000$  and  $\bar{M}_n = 56\,000$ . Both were dissolved in methyl ethyl ketone.

(4) Poly(styrene-methyl methacrylate) (PSMMA), a random copolymer consisting of 35% styrene and 65% methyl methacrylate,  $\bar{M}_w = 140\,000$  and  $\bar{M}_n = 74\,000$  dissolved in toluene.

A series of PS-PPO blends were also prepared, using 10, 25, 50, 75 and 90 wt% polystyrene (PS) mixed with the PPO used above. [The PS had  $\bar{M}_w = 300\,000$  and  $\bar{M}_n = 124\,000$  and contained none of the mineral oil commonly present in commercial grades.] These were dissolved in chloroform. Two further PS-PPO blends were prepared using 25 and 50 wt% polystyrene of low molecular weight,  $\bar{M}_w = 4000$  and  $\bar{M}_w/\bar{M}_n \leq 1.06$  with the same PPO. These blends were also dissolved in chloroform.

Polymer films were prepared by drawing glass slides from each solution at a constant rate. After drying, the polymer film was floated off the slide onto a water bath from which it was picked up on an annealed copper grid

which had previously been coated with a film of the same polymer.

Bonding of the film to the grid was achieved by a short exposure of the vapour of the same solvent. To introduce cracks of controlled geometry from which crazes or DZs may be preferentially nucleated, a method has been developed<sup>12</sup> using the intense beam of a JEOL 733 electron microprobe to 'burn' a thin slit of material. In this way, cracks typically 100–120  $\mu\text{m}$  long by  $< 10 \mu\text{m}$  wide could be introduced into the centre of each grid square. Typical operating conditions for the microscope were 25–30 keV and 30–150 nA.

After the generation of these cracks, grids were mounted in a strain frame and strained in air while being observed with an optical microscope. The growth of crazes and deformation zones could thus be followed as a function of time. After straining, suitable grid squares could be cut out and examined by TEM (a Siemens 102 electron microscope operating at 125 keV was used); the level of applied strain was maintained during this process via the copper grid which deforms plastically. The details of this specimen preparation procedure have been discussed by Lauterwasser and Kramer<sup>8</sup>.

To characterize the extension ratio of the DZs the method developed by Lauterwasser and Kramer<sup>8</sup> for obtaining the volume fraction,  $v_f$ , of fibrillar material within a craze may be used. For a craze,  $v_f$  is found from microdensitometry of the electron image plate from which values for the optical densities of the images of the craze ( $\phi_{craze}$ ), the film ( $\phi_{film}$ ), and of a hole through the film ( $\phi_{hole}$ ) are obtained. The value of  $v_f$  is then given by:

$$v_f = 1 - \frac{\ln(\phi_{craze}/\phi_{film})}{\ln(\phi_{hole}/\phi_{film})} \quad (2)$$

For DZs,  $v_f$  is the ratio of the thickness within the zone to the undeformed film thickness, and the appropriate expression is identical to equation (2) but with  $\phi_{craze}$  replaced by  $\phi_{DZ}$ , the optical density of the deformation zone image<sup>12</sup>. Since both crazing and DZ formation are plastic deformation processes which occur at constant polymer volume, the extension ratio  $\lambda$  is simply:

$$\lambda = 1/v_f \quad (3)$$

## RESULTS

Figure 1 shows the appearance of a typical DZ in annealed PPO. Other polymers show similar structures at crack tips—the complete absence of fibrillation distinguishing DZs from crazes. In Tables 1–3, average values for the extension ratios within the DZs are listed for the polymers investigated. These Tables also predict  $\lambda_{max}$  using equation (1) and the given values of  $l_e$  and  $d$ . For the homopolymers and copolymers the values of  $l_e$  were obtained from:

$$l_e = \frac{M_e}{M_0} l_0 \quad (4)$$

where  $M_e$  was determined from melt elasticity measurements<sup>14</sup> and  $l_0$ , the length of a fully-extended chain unit of molecular weight  $M_0$ , was obtained from crystallographic data<sup>15,16</sup>. The tabulated  $d$  values were

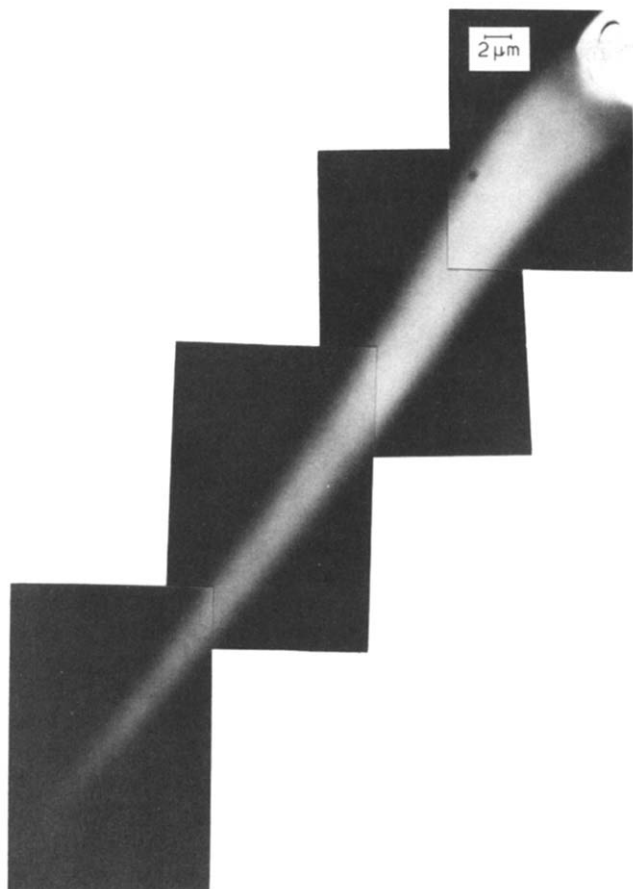


Figure 1 TEM micrograph of a deformation zone in PPO which had been annealed for 1 h at 100°C

Table 1 Parameters for homopolymers and copolymers

Polymer	$l_e$ (Å)	$d$ (Å)	$\lambda_{\max}$	$\lambda_{DZ}$	$\lambda_{\text{craze}}$
PC	110	44	2.5	1.4	2.0
PSAN2	180	67	2.7	1.8	2.0
PSMMA	190	61	3.1	1.7	2.0
PSAN1	270	82	3.3	2.0	2.7

computed as the root-mean-square end-to-end distance for a random polymer coil of molecular weight  $M_e$ , i.e.:

$$d = k(M_e)^{1/2} \quad (5)$$

The constant  $k$  was obtained from measurements of coil sizes for the polymer in a  $\theta$ -solvent<sup>17</sup>. Further discussion of the calculation of  $\lambda_{\max}$  is given in ref. 10.

For the PS-PPO blends the entanglement molecular weight was calculated from an equation derived by Prest and Porter (18):

$$M_e(\chi) = \frac{M_e(\text{PS})}{1 + 3.2\chi} \quad (6)$$

where  $\chi$  is the weight fraction of PPO in the blend. Assuming this equation is valid for all values of  $\chi$ , and taking the value of  $M_e(\text{PS})$  as 19 100<sup>14</sup>, yields  $M_e(\text{PPO}) = 4300$  and  $l_e = 165$  Å. Values of  $l_e$  for the blends can then be obtained from the equation:

$$l_e(\chi) = M_e(\text{PS}) \frac{(0.0209 + 0.0175\chi)}{1 + 3.2\chi} \quad (7)$$

which will be valid if a simple rule of mixtures is adequate to describe the variation in  $l_e/M_e$ . The entanglement mesh size,  $d$ , is 55 Å for PPO<sup>10</sup> and  $d$  for PS = 96 Å (obtained from equation 5 and small-angle neutron scattering experiments<sup>19</sup>). Linear interpolation is used to calculate the  $d$  values for the blends of high MW PS with PPO to give:

$$d(\chi) = 96 - 41\chi \quad (8)$$

and hence  $\lambda_{\max}$  may be found by combining equations (7) and (8).

For the two blends of PPO with PS of molecular weight 4000, which lies well below  $M_e = 19\,100$ , the PS chains cannot form part of the entanglement network, which will therefore be composed entirely of PPO chains. The correct values of  $l_e$  and  $d$  can be determined simply by allowing for the appropriate dilution of the PPO chains. Since the two components have markedly different molecular weights, the arguments of De Gennes<sup>20</sup> indicate that the short chains will act as a good solvent for the long chains causing them to expand relative to their random coil configuration in a  $\theta$ -solvent. This expansion will lead to a change in  $d$ :

$$d_G = d_\theta \chi^{-1/8} \quad (9a)$$

where  $d_G$  and  $d_\theta$  are the  $d$  spacings in a good and in a  $\theta$ -solvent respectively, and:

$$d_\theta = k[M_e(\chi)]^{1/2} \quad (9b)$$

The values of  $M_e$  and  $l_e$  scale as  $1/\chi$ . These equations lead to:

$$d_G(\chi) = \frac{d(\chi=1)}{\chi^{5/8}} \quad (9c)$$

Table 2 Parameters for high MW PS-PPO blends

$\chi$ (wt fraction PPO)	$l_e$ (Å)	$d$ (Å)	$\lambda_{\max}$	$\lambda_{DZ}$	$\lambda_{\text{craze}}$
0	400	96	4.2	—	4
0.1	330	92	3.6	2.3	3.6* 3.3
0.25	270	86	3.1	2.1	3.2
0.5	220	76	2.9	2.6* 2	3.4* 2.8
0.75	190	65	2.9	2.4* 1.6	2.9*
0.9	180	59	3.0	1.8*	2.7*
1.0	165	55	3.0	1.6*	2.6*

\* Denotes annealed specimen

Table 3 Parameters for low MW PS-PPO blends

$\chi$	$l_e$ (Å)	$d_G$ (Å)	$\lambda_{\max}$	$\lambda_{DZ}$	$\lambda_{\text{craze}}$
0.5	330	84	3.9	2.8	3.7
0.75	220	76	2.9	1.6	3.4

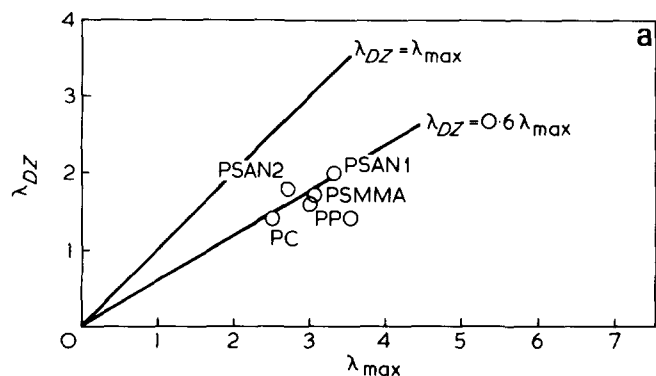


Figure 2a Measured values of  $\lambda_{DZ}$  plotted against the predicted value of  $\lambda_{max}$  for homopolymers and copolymers. Lines  $\lambda_{DZ} = 0.6 \lambda_{max}$  and  $\lambda_{DZ} = \lambda_{max}$  are shown

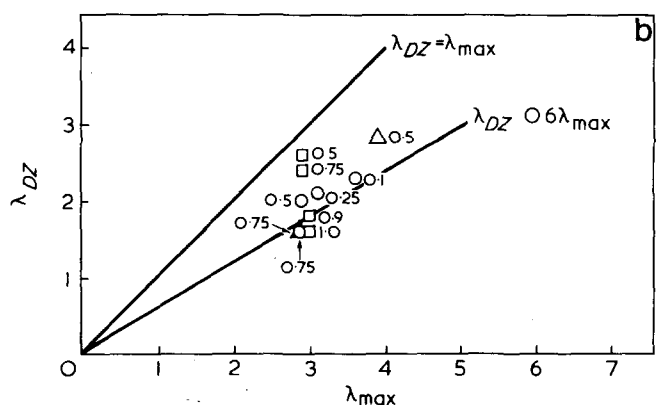


Figure 2b Measured values of  $\lambda_{DZ}$  plotted against the predicted value of  $\lambda_{max}$  for PS-PPO blends, points designated by:  $\circ$ , unaged specimens;  $\square$ , annealed specimens;  $\triangle$ , blend with low  $M_w$  PS

and

$$l_e(\chi) = \frac{l_e(\chi=1)}{\chi} \quad (9d)$$

$\lambda_{max}$  can be calculated for the blends from equations (9c) and (9d). Further discussion of the validity of these concepts for PS-PPO blends is given in ref. 11.

## DISCUSSION

From Tables 1-3 the values of  $\lambda_{DZ}$  determined experimentally can be compared with the predicted values of  $\lambda_{max}$ . It can be seen that  $\lambda_{DZ}$  follows the same trend as  $\lambda_{max}$  but lies systematically below it. This trend is shown more clearly in Figures 2a and 2b which are plots of  $\lambda_{DZ}$  versus  $\lambda_{max}$ . The points cluster about the line  $\lambda_{DZ} = 0.6 \lambda_{max}$  which is also shown in Figure 2. Tables 1-3 also indicate that the measured  $\lambda_{DZ}$  values always lie below  $\lambda_{craze}$ .

From these results it is clear that the entanglement network is also of fundamental importance in determining the 'natural draw ratio' of deformation zones, just as it is for crazes. Since crazing and DZ growth are competitive processes, we wish to identify those parameters which determine which mode of deformation occurs and how the response of the entanglement network differs for the two modes.

Only those polymers with low  $l_e$  values exhibit DZs. Because strain hardening sets in at relatively low strains

for these polymers, the tendency for any locally deforming region to become a craze is suppressed<sup>10</sup>. Polycarbonate, PC, which has the shortest  $l_e$  of any of the systems under investigation, rarely shows crazing, whereas PS never exhibits DZs in these films. A more systematic study of the changing nature and occurrence of DZs with  $l_e$  is possible by examining the behaviour of polymers in the series of PS-PPO blends.

When pure, unaged, PPO is strained, diffuse deformation zones form, reminiscent of those seen in PC<sup>12</sup>, (Figure 3). For these zones,  $\lambda$  varies both along and across the zone, as revealed by the thickness interference fringes formed when these zones are viewed under monochromatic light in a reflected-light microscope. Crazes are never seen in unannealed films of PPO.

After pure PPO has been annealed at temperatures in the range 80°-170°C, the zones become localized with an extension ratio essentially constant throughout the zone, permitting a well-defined  $\lambda_{DZ}$  to be measured. The value so measured is little altered by either the time or temperature of the annealing treatment, although there is a slight increase in  $\lambda$  upon long time-high temperature annealing. In contrast to the behaviour of annealed PC, crazes as well as DZs form in aged PPO. In general DZs grow rapidly from crack tips. At longer times under the constant strain conditions in these films, fibrillation starts to occur at the edges of the DZ and also, if the zone continues to propagate, at its tip. The changing nature of the deformation can be observed optically during growth and the final DZ/craze microstructure may be characterized by TEM. An example is shown in Figure 4. Isolated crazes also grow slowly in other parts of the film. Thus, the mechanism of fibrillation apparently requires a longer time scale than the shear process involved in DZ growth.

As the ratio of PPO to PS in the blend series is decreased, a change in the form of the DZs which grow from crack tips in unannealed films may be observed. There is a gradual transition from the diffuse DZ of pure PPO, to a relatively well-defined (constant  $\lambda_{DZ}$ ) DZ with sharp edges in 25% PPO blends, to no DZs at all but only crazes in 100% PS films. Those blends ( $\geq 50\%$  PPO) that form relatively diffuse zones in unaged films form localized DZs at crack tips upon annealing as well as exhibiting an increased tendency for crazing. Those blends (10-50% PPO) that show localized DZs without annealing also show an increased tendency to form crazes upon annealing. For example, a 10% PPO-PS blend shows crazing only after an ageing treatment. The tabulated values of  $\lambda_{DZ}$  given in Tables 2 and 3 refer to

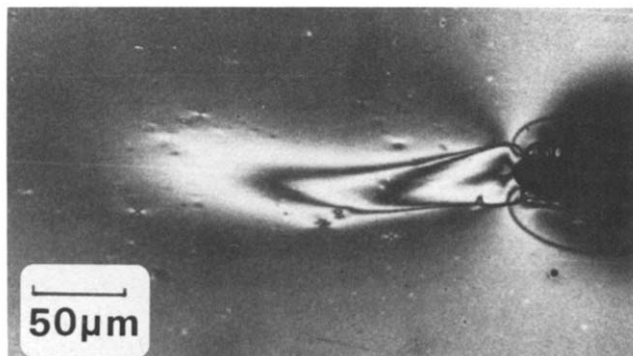


Figure 3 Diffuse DZ in the higher molecular weight PPO



Figure 4 Growth of crazes at the edges of a zone in a PPO film which had been annealed for 2 h at 132°C

measurements on zones which are localized and have a well-defined and constant value for  $\lambda$  over the majority of their lengths.

A clear example of how closely connected the unvoided structure of the *DZ* is to the typical craze structure can be seen in Figure 5 which shows the region at a crack tip in a 50% PPO-PS blend annealed for 1.5 h at 100°C. The appearance shows how intimately related the two processes are, with short segments of 'craze' interspersed with unvoided polymer, and with the 'proportion of craze' increasing towards the edge of the zone where the thickening rate is slow. A similar hybrid deformation zone, in which short regions of craze are interspersed with and border on a drawn but unfibrillated *DZ*, has also been observed in PSMMA.

In the model for calculating  $\lambda_{\max}$  it is assumed that the network entanglement points behave as permanent crosslinks during deformation, with neither chain slippage via reptation nor scission altering this network. To generate the void-fibril network of a craze, however, some degree of chain scission and/or slippage must occur. Chains that are entangled on either side of what will become a fibril surface must either disentangle or break. For growth of the unvoided *DZ*, chain scission and/or chain disentanglement are not necessary and are likely to be much less important.

This hypothesis at once qualitatively rationalizes why  $\lambda_{DZ}$  is always lower than  $\lambda_{\text{craze}}$  in the same polymer or blend. The chain scission or disentanglement necessary for fibrillation to occur in the craze also modifies the entanglement network sufficiently to increase the ultimate extension ratio. Furthermore, since chain

disentanglement (reptation) is closely related to the self-diffusion of the polymer chains, it is logical to expect that its contribution to deformation will increase with time under stress with a consequent increase in craze formation. This hypothesis is in accord with the experimental facts. Based on these arguments one would also expect a *DZ* to craze transition as the rate of straining is decreased. Preliminary evidence suggests that this is so.

The role of chain scission is harder to assess. The observation that  $\lambda_{\text{craze}}$  for poly(*t*-butylstyrene) exceeds  $\lambda_{\max}$  suggests for polymers with high  $\lambda$ s and therefore high fibril true stresses, scission will become important. The damage that a single scission provokes will be related to the molecular weight of the chains; a broken short chain will be more prone to disentanglement via reptation, leading to fibril breakdown.

To test for such a molecular weight effect a second PPO resin was used with  $M_w = 197\,000$  and  $\bar{M}_n = 105\,000$ . Whereas the  $\bar{M}_w$  of the lower PPO ( $\bar{M}_w = 35\,000$ ) chain was significantly larger than  $M_e$  for PPO, the average number of entanglement points per chain was relatively low ( $\sim 8$ ). The fragility of the resulting entanglement network was particularly noticeable in the blends of this PPO with low *MW* PS<sup>11</sup>, resulting in short weak crazes which rapidly broke down to form cracks. In contrast to this behaviour, blends of PPO ( $\bar{M}_w = 197\,000$ ) with 66% low molecular weight PS were much more stable, with longer crazes being formed which did not fail.

A second experiment also demonstrates how craze breakdown is related to chain scission for chains with few entanglement points. When a film of the lower  $M_w$  PPO was annealed for 1.5 h at 174°C, both crazes and *DZ*s were formed on subsequent straining. After 5 days under strain, breakdown of a few of both the crazes and the *DZ*s at crack tips was observed. Examination of the microstructure of the remaining crazes showed evidence that these too had probably broken down, with retracted fibrils present at the craze edges (Figure 6). Measurement of the 'extension ratio' at different points across the craze confirmed that the value at the craze edge fell below the average  $\lambda_{\text{craze}}$  value whereas the region where the fibrils had failed lay above these values for fresh PPO crazes. In contrast to this behaviour, a film of the high  $M_w$  PPO annealed and strained in the same way showed no sign of craze or *DZ* breakdown.

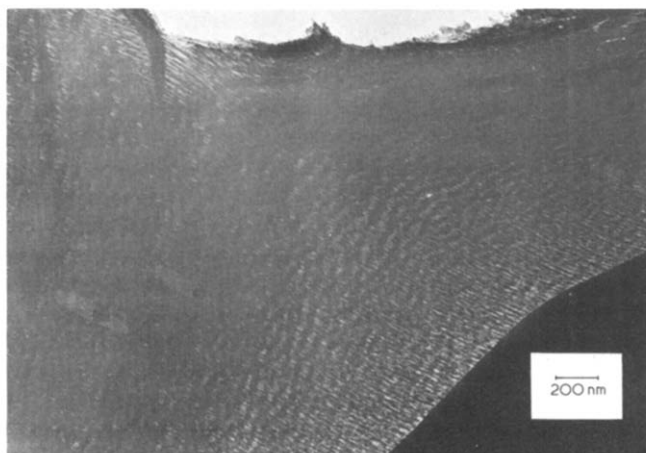


Figure 5 Short segments of 'craze' interspersed with unfibrillated polymer in a 50-50 PS-PPO blend annealed for 1 h at 100°C

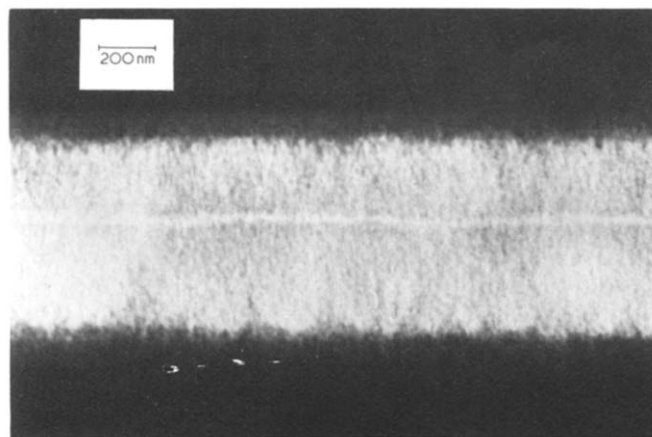


Figure 6 Appearance of a partly failed craze in PPO annealed for 1.5 h at 174°C and left under strain for 5 days

Craze breakdown in this fashion is most likely to occur for a film that has been severely annealed because the increase in modulus leads to higher fibril true stresses at a given strain level and hence a greater probability of failure. It is probably for this reason that there is a slight increase in  $\lambda_{DZ}$  (as mentioned above) for highly annealed films of PPO. Similarly, this argument explains why  $\lambda_{DZ}$  for the 50% PPO-PS and 75% PPO-PS blends (which must be annealed to produce well-defined DZs) lie significantly above the line  $\lambda_{DZ}=0.6 \lambda_{max}$  which characterizes  $\lambda_{DZ}$  in the other polymers reasonably accurately (Figure 2).

## CONCLUSIONS

These experiments demonstrate the following important points:

(1) Deformation zones are observed for polymers and polymer blends which have low values of  $l_e$ , but not for those which have high  $l_e$  values;

(2) For DZs, as for crazes, the extension ratio within the zone is largely governed by the  $\lambda_{max}$  of the entanglement network of the polymer; typically  $\lambda_{DZ}=0.6 \lambda_{max}$ ;

(3) In polymers in which DZs and crazes both occur, DZs tend to form rapidly whereas crazes appear only after long times;

(4) The fact that a certain degree of chain scission/chain disentanglement (both kinetic processes) is necessary for

craze fibrillation accounts for both the delayed appearance of crazes relative to DZs and the fact that  $\lambda_{craze}$  is always higher than  $\lambda_{DZ}$  in the same polymer.

## ACKNOWLEDGEMENTS

The financial support of the US Army Research Office, Durham, is gratefully acknowledged. This research has also benefited from the use of the facilities of the Corning Materials Science Center which is funded by the National Science Foundation. We would like to thank Dr Robert Bubeck for supplying us with the PS, PSAN and PSMMA and Dr Roger Kambour for the supply of the PC and PPO resins.

## REFERENCES

- 1 Kambour, R. P. *J. Polym. Sci. (D)* 1973, **7**, 1
- 2 Rabinowitz, S. and Beardmore, P. *Crit. Reviews Macromol. Sci.* 1972, **1**, 1
- 3 Gent, A. N. in 'The Mechanics of Fracture', AMD Vol. 19, (Ed. F. Erdogan), ASME, MY, 1976, p. 55
- 4 Kambour, R. P. and Holik, A. S. *J. Polym. Sci. (A-2)* 1969, **7**, 1393
- 5 Beahan, P., Bevis, M. and Hull, D. *Phil. Mag.* 1971, **24**, 1267
- 6 Beahan, P., Bevis, M. and Hull, D. *Proc. Roy. Soc. London (A)* 1975, **343**, 525
- 7 Wellinghoff, S. and Baer, E. *J. Macromol. Sci. (B)* 1975, **11**, 367
- 8 Lauterwasser, B. D. and Kramer, E. J. *Phil. Mag. (A)* 1979, **39**, 469
- 9 Donald, A. M., Chan, T. and Kramer, E. J. *J. Mater. Sci.* 1981, **16**, 669
- 10 Donald, A. M. and Kramer, E. J. *J. Polym. Sci., Polym. Phys. Edn.* in press; (Cornell University MSc Report 4407)
- 11 Donald, A. M. and Kramer, E. J. *Polymer* 1981, **22**, 461; (Cornell University MSc Report 4491)
- 12 Donald, A. M. and Kramer, E. J. *J. Mater. Sci.* 1981, **16**, 2967 (Cornell University MSc Report 4331)
- 13 Donald, A. M. and Kramer, E. J. *J. Mater. Sci.* 1981, **16**, 2977 (Cornell University MSc Report 4371)
- 14 Seitz, J. T. 'Measurements of Entanglement Length in Broad Molecular Weight Systems', presented at the 50th Golden Jubilee of the Rheology Society, Boston, MA, 1979, to be published
- 15 Vincent, P. I. *Polymer* 1972, **13**, 558
- 16 Miller, R. L. in 'Polymer Handbook', (Eds. J. Brandrup and E. H. Immergut), Wiley, New York, 1975, III-1
- 17 Kurata, M., Tsunashima, Y., Iwama, M. and Kamada, K. *ibid.* IV-4
- 18 Prest, W. M. and Porter, R. S. *J. Polym. Sci. (A-2)* 1972, **10**, 1639
- 19 Kirste, R. G., Kruse, W. A. and Ibel, K. *Polymer* 1975, **16**, 120
- 20 DeGennes, P. G. 'Scaling Concepts in Polymer Physics', Cornell University Press, Ithaca, NY, 1979